Multipath Assisted Positioning in Vehicular Applications

Markus Ulmschneider, Ronald Raulefs, Christian Gentner and Michael Walter

***Abstract*—Precise localization and tracking in intelligent transportation systems has aroused great interest since it is required in a large variety of applications. The positioning accuracy of global navigation satellite systems is unreliable and insufficient enough for many use cases. In urban canyons or tunnels, the positioning performance degrades due to a low received signal power, multipath propagation, or signal blocking. Instead we exploit the ubiquitous access to cellular mobile radio networks. Cellular networks are designed to cover the access to the network in an area by a single link to reduce the risk of interference from neighboring base stations. The idea of Channel-SLAM is to exploit the numerous multipath components (MPCs) of a radio signal arriving at the receiver for positioning. Each MPC can be regarded as being sent from a virtual transmitter in a pure line-of-sight condition. Within this paper, we show how to apply multipath assisted positioning in an urban scenario. Therefore, we analyze how a road user equipped with a circular antenna array is tracked in an urban scenario in the presence of only one physical transmitter. We further jointly estimate the positions of the physical and the virtual transmitters to enrich maps.**

***Index Terms*—Channel-SLAM, multipath assisted positioning, simultanous localization and mapping, tracking**

I. Introduction

The rapid growth of available services and applications depending on location awareness in intelligent transportation systems (ITSs) has led to an ever increasing demand for precise localization and tracking systems. Examples for these applications range from enhanced navigation with guided lane tracking, and platooning to fully autonomous driving.

The positioning accuracy of global navigation satellite systems (GNSSs) is not sufficient for many applications. Furthermore, certain scenarios such as urban canyons or tunnels pose an additional challenge due to multipath propagation and blocking of signals [1]. Hence, especially in such areas, there is a high demand for complementary positioning systems.

There exists a variety of systems that may be used to support GNSS in such challenging scenarios. They include radar or lidar, as well as optical systems. Radar and lidar are usually used for relative positioning among surrounding traffic, but they can not see through surrounding traffic or beyond blocking objects (walls, etc.). However, optical systems may be used for relative positioning, but also for absolute positioning if a-priori information in form of a map based on visual features is available. Different weather and daylight conditions pose severe challenges to such systems.

In tunnels or urban canyons, a rich multipath environment can be expected [2]. Multipath propagation has been considered a foe using wireless positioning and navigation technologies, since it biases range estimates and hence degrades the positioning accuracy. Standard methods to tackle the multipath problem estimate the channel impulse response (CIR) at a receiver that has to be located, and try to mitigate the influence of the multipath components (MPCs) on the line-of-sight (LoS) path.

Our proposed approach is to use a radio frequency (RF) based system that is based on multipath assisted positioning using signals of opportunity (SoO). Contrary to the standard methods, the idea of multipath assisted positioning is not to combat MPCs, but to exploit them for positioning: each MPC arriving at a receiver via a different propagation path can be regarded as a separate signal being sent synchronously from another signal source in a pure LoS condition to the receiver. We name such a signal source a virtual transmitter (VT). The concept of VTs will be explained in more detail in Section II. Both the physical and the virtual transmitters can be used for positioning.

Fundamental limits and theoretical results on multipath assisted positioning have been presented in [3]. Some approaches using multipath assisted positioning assume the physical and virtual transmitter positions to be known in advance, for example in form of a floorplan in indoor [4] or in radar [5] applications.

In a general setting, however, the positions of the virtual and possibly also of the physical transmitters are unknown. Their positions might be estimated jointly with the receiver position in a simultaneous localization and mapping (SLAM) algorithm as the receiver travels through the scenario. In this respect, locating the receiver and mapping the physical and virtual transmitters is performed simultaneously. With the Channel-SLAM algorithm, an approach has been presented in [6], [7] that uses a recursive Bayesian estimation approach for the estimation problem. The algorithm does not differentiate between physical and virtual transmitters: each signal component arriving at the receiver, no matter if via the LoS path or as a MPC, is treated as a signal from a transmitter in a pure LoS condition.

Today's local dynamic maps (LDMs) for ITS applications contain data that support localization to improve the control functions of the vehicle. The inclusion of additional features to LDMs, such as virtual or physical transmitter locations, might support systems using such maps and improve the positioning performance. Moreover, it increases the reliability under conditions where not enough physical transmitters are present.

The purpose of this paper is to show how to use multipath assisted positioning in vehicular applications. We simulate a

The authors are with the Institute of Communications and Navigation of the German Aerospace Center (DLR), Muenchner Str. 20, 82334 Wessling, Germany. (e-mail: {markus.ulmschneider,ronald.raulefs,christian.gentner,m.walter}@dlr.de)

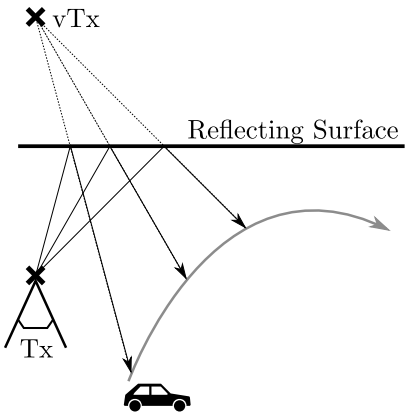

Fig. 1. Signals from the physical transmitter Tx are reflected at the straight surface and can be interpreted as originating from a VT vTx, which is static during the receiver motion. The position of vTx is the position of the physical transmitter Tx mirrored at the surface.

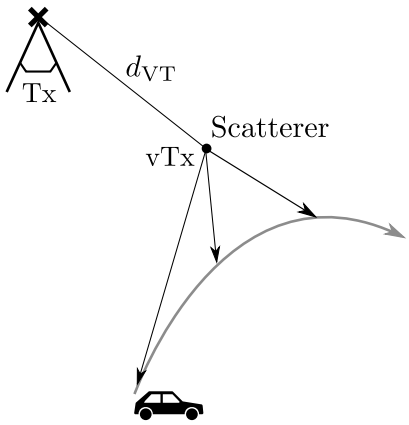

Fig. 2. Signals from the physical transmitter Tx are scattered at the punctual scatterer and can be interpreted as originating from a VT vTx, which is static during the receiver motion. The VT has an additional propagation distance d_{VT} compared to the physical transmitter Tx.

road user moving through an urban environment. The user is equipped with a gyroscope and a circular antenna array in order to be able to incorporate angle of arrival (AoA) information of incoming signal components.

The remainder of the paper is organized as follows. Section II introduces the idea of multipath assisted positioning and its application in a vehicular context. The Channel-SLAM algorithm is derived in Section III. We present the simulation scenario and results in Section IV. Section V concludes the paper.

II. Multipath Assisted Positioning

The Channel-SLAM algorithm uses MPCs for positioning instead of mitigating them. In order to use MPC for positioning, a model reflecting the MPCs parameters in dependency of the receiver position needs to be found. Channel-SLAM treats each MPC as a LoS signal from a VT whose position is unknown to the receiver.

Fig. 1 illustrates the idea of VTs: The physical transmitter Tx broadcasts a signal that arrives via a reflection from a straight surface, i.e. via a non-line-of-sight (NLoS) path. From the user point of view, this signal may be regarded as being sent from the VT vTx in a pure LoS condition. The position of the VT is the position of the transmitter Tx mirrored at the surface. As the user moves along its trajectory, the position of the VT is static and the VT is inherently synchronized to the physical transmitter.

Fig. 2 presents a scenario where the signal is scattered. The propagation effect of scattering occurs if an electromagnetic wave impinges an object and the energy is spread out in all directions. If the receiver moves through this scenario, the signals scattered from this punctual scatterer seem to be emerging from the scatterer itself. Hence, we obtain a VT at the scatterer position. This VT, however, has an additional clock offset $\tau_{\mathrm{VT}} > 0$ towards the physical transmitter. In Fig. 2, τ_{VT} is the propagation distance between the physical and the VT, d_{VT}, divided by the speed of light. A transmitter's clock offset and its additional propagation time are therefore equivalent.

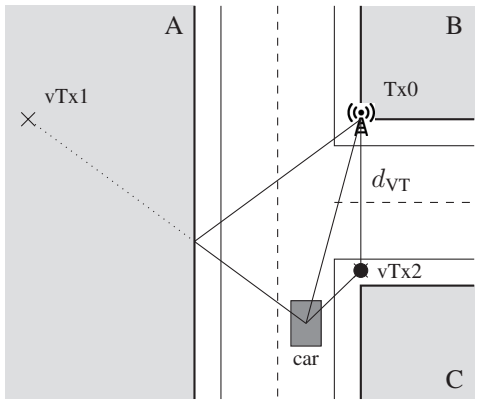

Fig. 3. A car moves from the bottom to the top through an urban scenario with three buildings A, B, and C. The physical transmitter Tx0 is located at the corner of building B. There are two MPCs arriving at the receiver that are regarded as being transmitted by the VTs vTx1 and vTx2.

Between the physical transmitter and the scatterer additional interactions are possible. Hence, the concepts of single reflections and single scatterings can be generalized in a straightforward manner to situations where a signal from a physical transmitter undergoes multiple reflections and scatterings [6], [7]. The propagation path of each MPC can therefore be equivalently described as a direct path between a VT and the receiver plus a constant additional propagation distance d_{VT}. If only reflections occur on the pathway between physical transmitter and receiver, this additional propagation distance is zero. If the MPC was interacting with at least one scatterer, the additional propagation distance is greater than zero.

A scenario of a car equipped with an RF receiver moving through an urban canyon is depicted in Fig. 3. The driving direction of the car is from bottom to the top. The light gray areas represent walls of buildings reflecting RF signals, and the buildings are labeled A, B, and C. A physical transmitter, labeled Tx0, is located at the corner of building B. The transmitter might be emitting radio signals. The car is in LoS to Tx0. One MPC arrives at the car via the reflection at the wall of building A. Following the Channel-SLAM concept,

this MPC can be regarded as being sent from the VT vTx1 in a pure LoS condition. The position of vTx1 is the position of the physical transmitter Tx0 mirrored at the wall of building A. The black circle near the corner of building C models a punctual scatterer. One signal component at the car is received via this scatterer. Hence, the scatterer can be regarded as an additional VT vTx2 as in Fig. 2. Accordingly, the position of vTx2 is equal to the position of the punctual scatterer, and its additional propagation distance d_{VT} to the receiver is the Euclidean distance between Tx0 and Tx2.

III. Algorithm Derivation

A propagation path can be represented by a direct path between a VT and the receiver. Hence, for each MPC i, with $i = 0, \ldots, N(t_k) - 1$, we can define a VT by its position $\boldsymbol{r}_{\mathrm{VT},i}(t_k)$ and an additional propagation distance $d_{\mathrm{VT},i}(t_k)$, where $N(t_k)$ is the number of MPCs, or equivalently, VTs, at time instant t_k. Knowing the positions of the VTs, the receiver position $\boldsymbol{r}_u(t_k)$ can be estimated. A method to estimate the position of the receiver at the same time as landmarks located in the environment is called SLAM [8]. We consider a stationary scenario with a moving receiver. The SLAM algorithm is used by the receiver to estimate its own position and the position of the VTs as landmarks.

In a first step, the received signal is processed by the Kalman enhanced super resolution tracking (KEST) algorithm [9], which estimates for each MPC i the propagation length $d_i(t_k)$, the complex amplitude $\alpha_i(t_k)$ and the AoA $\phi_{a,i}(t_k)$ in the azimuth plane as shown in Fig. 4. Our approach considers a 2.5-dimensional scenario, and the antenna array is able to measure the azimuth and the elevation angle. However, within the scope of this paper, we consider a 2-dimensional positioning approach, and hence, only the azimuth angle is considered. For each time instant t_k, the relevant estimates of the KEST algorithm are condensed as the vector $\mathbf{z}(t_k)$ with

$$\mathbf{z}(t_k) = [\hat{\boldsymbol{\phi}}_a(t_k)\ \hat{\mathbf{d}}(t_k)], \tag{1}$$

where

$$\hat{\boldsymbol{\phi}}_a(t_k) = [\hat{\phi}_{a,0}(t_k),\ \ldots\ , \hat{\phi}_{a,N(t_k)-1}(t_k)]^T \tag{2}$$

are the estimates for the AoA in the azimuth plane and

$$\hat{\mathbf{d}}(t_k) = [\hat{d}_0(t_k),\ \ldots\ , \hat{d}_{N(t_k)-1}(t_k)]^T \tag{3}$$

are the estimates for the propagation lengths.

In order to use the VTs for positioning, their states have to be estimated during the receiver movement. Hence, the state vector $\mathbf{x}(t_k)$ at time instant t_k is defined by

$$\mathbf{x}(t_k) = \left[\mathbf{x}_u(t_k)^T, \mathbf{x}_{\mathrm{VT},0}(t_k)^T, \ldots, \mathbf{x}_{\mathrm{VT},N(t_k)-1}(t_k)\right]^T, \tag{4}$$

with the receiver state

$$\mathbf{x}_u(t_k) = \left[\boldsymbol{r}_u(t_k)^T, \boldsymbol{v}_u(t_k)^T, b_u(t_k), \rho_u(t_k)\right]^T, \tag{5}$$

where $\boldsymbol{r}_u(t_k)$ is the receiver position, $\boldsymbol{v}_u(t_k)$ the receiver velocity, $b_u(t_k)$ and $\rho_u(t_k)$ the receiver's clock bias and drift, respectively. The parameters representing the VT of the i^{th} MPC are defined as

$$\mathbf{x}_{\mathrm{VT},i}(t_k) = \left[\boldsymbol{r}_{\mathrm{VT},i}(t_k)^T, d_{\mathrm{VT},i}(t_k)\right]^T, \tag{6}$$

where $\boldsymbol{r}_{\mathrm{VT},i}(t_k)$ is the position of the i^{th} VT and $d_{\mathrm{VT},i}(t_k)$ its additional propagation distance.

For solving the SLAM problem, i.e., estimating the state vector $\mathbf{x}$ at time steps 0 to k, $\mathbf{x}(t_{0:k})$, we follow a recursive Bayesian filtering approach. In general, recursive Bayesian filtering provides a methodology to optimally estimate parameters in non-stationary conditions [10]. It consists of two steps, the prediction step and the update step. As illustrated in [7], assuming a first-order Markov model and independence among the measurements for the single VTs, the transition prior can be expressed here as

$$\begin{aligned}\mathsf{p}\big(\mathbf{x}(t_k)|\mathbf{x}(t_{k-1})\big) =& \mathsf{p}\big(\mathbf{x}_u(t_k)|\mathbf{x}_u(t_{k-1})\big) \\ &\cdot \prod_{i=0}^{N(t_k)-1} \mathsf{p}\big(\mathbf{x}_{\mathrm{VT},i}(t_k)|\mathbf{x}_{\mathrm{VT},i}(t_{k-1})\big),\end{aligned} \tag{7}$$

where the number of VTs at time t_k is denoted by $N(t_k)$. As mentioned in Section II and [7], the position of the VTs are time-invariant. Hence, we obtain for the i^{th} MPC

$$\mathsf{p}\big(\mathbf{x}_{\mathrm{VT},i}(t_k)|\mathbf{x}_{\mathrm{VT},i}(t_{k-1})\big) = \delta\left(\mathbf{x}_{\mathrm{VT},i}(t_k) - \mathbf{x}_{\mathrm{VT},i}(t_{k-1})\right). \tag{8}$$

For the transition prior probability density function (PDF) of the user state $\mathbf{x}_u(t_k)$, $\mathsf{p}\big(\mathbf{x}_u(t_k)|\mathbf{x}_u(t_{k-1})\big)$, we include gyroscope measurements for heading information. As shown in Fig. 4, the proposed movement model considers a two dimensional Cartesian coordinate system, where we obtain the heading changes $\Delta_\beta(t_k)$ from the gyroscope [11]. Hence, the receiver position $\boldsymbol{r}_u(t_k)$ is calculated as

$$\boldsymbol{r}_u(t_k) = \boldsymbol{r}_u(t_{k-1}) + (t_k - t_{k-1})\, \boldsymbol{v}_u(t_k)\,, \tag{9}$$

with the receiver velocity

$$\boldsymbol{v}_u(t_k) = \mathbf{R}(\Delta_\beta(t_k)) \cdot \boldsymbol{v}_u(t_{k-1}) + \mathbf{n}_u(t_k), \tag{10}$$

where $\mathbf{n}_u(t_k) \sim \mathcal{N}(0, \mathbf{Q}_u(t_k))$ is the transition noise with covariance matrix $\mathbf{Q}_u(t_k)$. The 2-dimensional rotation matrix $\mathbf{R}(\Delta_\beta(t_k))$ is

$$\begin{aligned}&\mathbf{R}(\Delta_\beta(t_k)) = \\ &\begin{bmatrix}\cos\left(\Delta_\beta(t_k) + n_\beta(t_k)\right) & -\sin\left(\Delta_\beta(t_k) + n_\beta(t_k)\right) \\ \sin\left(\Delta_\beta(t_k) + n_\beta(t_k)\right) & \cos\left(\Delta_\beta(t_k) + n_\beta(t_k)\right)\end{bmatrix},\end{aligned} \tag{11}$$

where $n_\beta(t_k)$ is the heading noise which is distributed following a von Mises distribution. For the clock bias and clock drift, known prediction models can be applied, see e.g. [12].

Assuming the elements of $\mathbf{z}(t_k)$ to be independent Gaussian distributed, the PDF $\mathsf{p}\big(\mathbf{z}(t_k)|\mathbf{x}(t_k)\big)$ for the update step of the

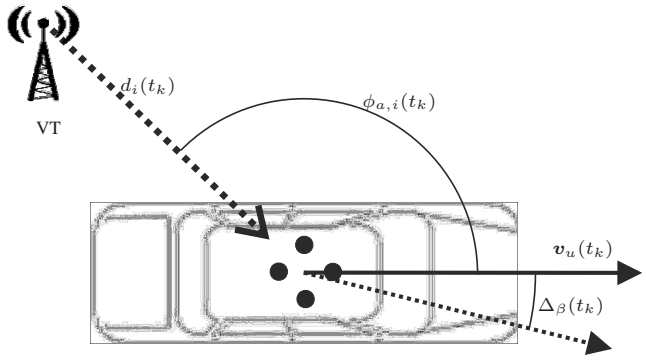

Fig. 4. A vehicle equipped with a circular antenna array that is visualized by the black dots. The antenna array is considered to be aligned in moving direction, and the center of the antenna array is defined as the phase center.

Bayesian filter can be expressed as

$$\mathrm{p}\big(\mathbf{z}(t_k)|\mathbf{x}(t_k)\big) = \prod_{i=0}^{N(t_k)-1} \frac{1}{\sqrt{2\pi}\sigma_{d,i}(t_k)} e^{-\frac{(\hat{d}_i(t_k)-d_i(t_k))^2}{2\sigma^2_{d,i}(t_k)}} \cdot \frac{1}{\sqrt{2\pi}\sigma_{\phi,a,i}(t_k)} e^{-\frac{(\hat{\phi}_{a,i}(t_k)-\phi_{a,i}(t_k))^2}{2\sigma^2_{\phi,a,i}(t_k)}}, \tag{12}$$

where $\sigma^2_{d,i}(t_k)$ and $\sigma^2_{\phi,a,i}(t_k)$ denote the corresponding noise variances of the additional propagation length and AoA measurements, respectively. The predicted propagation lengths $d_i(t_k)$ are calculated as

$$d_i(t_k) = \|\boldsymbol{r}_u(t_k) - \boldsymbol{r}_{\mathrm{VT},i}(t_k)\| + d_{\mathrm{VT},i}(t_k) + b_u(t_k)\cdot c, \tag{13}$$

where c denotes the speed of light. The predicted AoAs in the azimuth plane, $\phi_{a,i}(t_k)$, can be calculated as

$$\phi_{a,i}(t_k) = \mathrm{atan2}(\boldsymbol{r}_{\mathrm{VT},i}(t_k) - \boldsymbol{r}_u(t_k)) - \mathrm{atan2}(\boldsymbol{v}_u(t_k)), \tag{14}$$

where the function $\mathrm{atan2}(\mathbf{x})$ is the four quadrant inverse tangent function. It returns the angle between the positive x-axis and the point $\mathbf{x}$, which is positive for counter-clockwise angles. The AoAs are aligned in moving direction of the car as in Fig. 4, where the center of the antenna array is defined as the phase center.

IV. Simulations

For verifying our estimation approach, we performed simulations exploiting the multipath propagation in a simple urban scenario depicted in Fig. 5. The black lines represent walls reflecting the transmit signals, whereas black dots represent scattering objects. We have one physical transmitter, Tx0, that is represented by a red upward triangle. Knowing the environment, we model VTs that arise due to reflections and scattering of the signals emitted by Tx0 as illustrated in Section II. We incorporate reflections and scattering of orders one and two, i.e., single and double reflections and/or scattering.

Based on the positions of the physical and modelled virtual transmitters, we create a CIR for each time instance. We assume a power loss of 3 dB whenever a signal is reflected at a wall, and a power loss of 6 dB when the signal is scattered at a punctual scatterer. The CIRs are band-limited to a bandwidth of 100 MHz. Additionally, we add noise of a constant variance on top of the CIRs to reach an average signal-to-noise-ratio (SNR) of 7 dB.

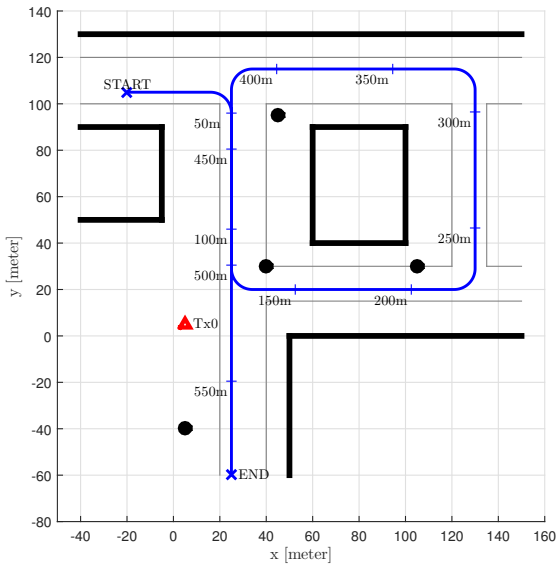

Fig. 5. An urban scenario with one physical transmitter labelled Tx0. The receiver track is depicted in blue with the start and end positions marked as START respectively END. The traveled distance is marked for every 50 m. Black lines represent walls that reflect the RF signal, black dots represent objects that scatter the signal.

As depicted in Fig. 4, the user is equipped with a 2-dimensional circular antenna array consisting of 4 antennas. It moves on a track represented in Fig. 5 by the blue line with a constant velocity of 10 m/s. The start and end positions are indicated by the labels START respectively END. The user starts moving to the right, takes a turn to the right moving downwards, turns left doing one loop around the central building and moves to its final position. During the user movement, the physical and virtual transmitters might be visible or not depending on the geometry of the scenario and the current user position. Hence, not all transmitters are visible at every user position.

The KEST algorithm estimates the parameters of the MPCs based on the sampled, band-limited CIRs, i.e., the received signal, every 0.05 ms. Fig. 6 shows the estimation results of KEST versus the receiver traveled distance in meters. The y-axis shows the delay of signal components arriving at the receiver. For the sake of a better intuition, the actual delays are multiplied by the speed of light resulting in values in meters, or, in other words, in propagation distances. Since Channel-SLAM considers an underdetermined system, long visible paths are preferable. For the evaluations, we extract only the long visible paths from the KEST estimates as visualized in Fig. 6. Although we could use all detected MPCs in Channel-SLAM, this would drastically increase the computational complexity.

Equivalently to [7], for the simulations, we implemented a Rao-Blackwellized particle filter (PF), see [13], that estimates

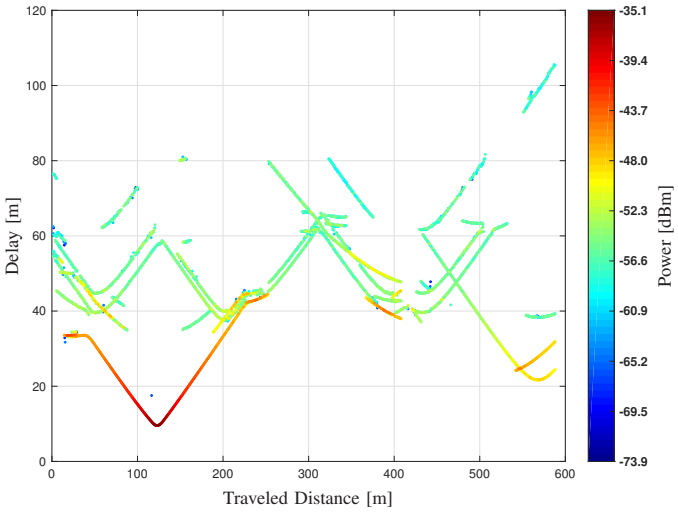

Fig. 6. Estimation results of KEST for the CIR versus the receiver traveled distance in meters. Only paths that are visible to the receiver for longer time are shown.

TABLE I
PARAMETERS OF THE USED SIGNALS

Parameter	Value
RF carrier frequency	1.51 GHz
signal bandwidth	100 MHz
average SNR	7 dB
measurement update rate	20 Hz

the user position and the location of the VTs as described in Section III. Accordingly, we simulate a gyroscope at the user, whose heading measurements are taken into account in the movement model of the receiver, again as mentioned in Section III.

We assume the starting position and the initial direction of the user to be known in order to define a local coordinate system. For its tracking, 3000 particles are initialized normally distributed around the true user position with a standard deviation of 1 m. We assume no a-priori knowledge on the physical and virtual transmitter positions and clock offsets. Hence, during the receiver movement, the VT states are estimated including the physical transmitter state. A new VT is initialized after KEST initializes a new propagation path. The initialization of a VT is performed based on the first AoA and propagation length measurements for this VT, i.e., the KEST estimates from Eq. (1), as in [7].

Fig. 7 shows an example of the estimated receiver trajectory by the cyan line. The figure also shows the PDFs of an estimated VT and the receiver position for a traveled distance of 245 m. The true position of the receiver is depicted by the blue cross. The PDF for the VT position is located close to the true physical transmitter position, and therefore corresponds most probably to the LoS path.

Fig. 8 shows the root mean square error (RMSE) for the user position versus the traveled distance. Because of using prior knowledge for the initialization of the receiver position, the position error at the beginning of the track is rather

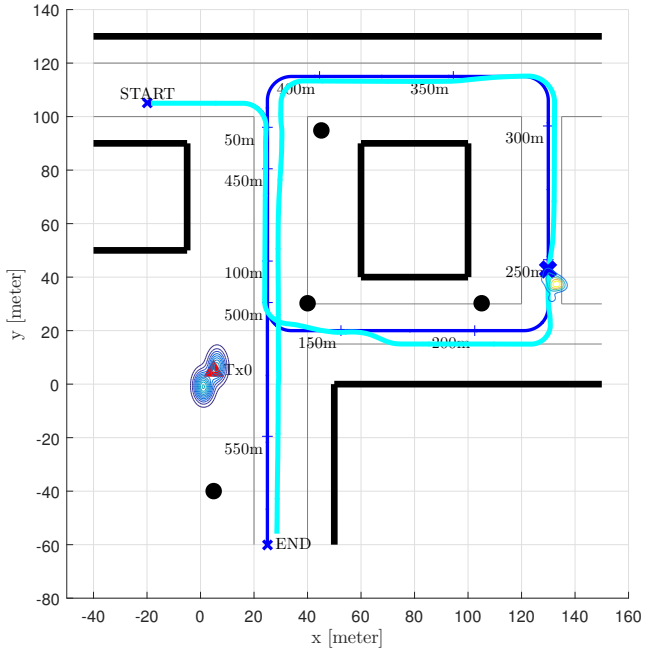

Fig. 7. Example estimated receiver trajectory in cyan. The blue track is the true receiver trajectory. Additionally, the PDFs of estimated VT positions and the receiver position for a traveled distance of 245 m are plotted.

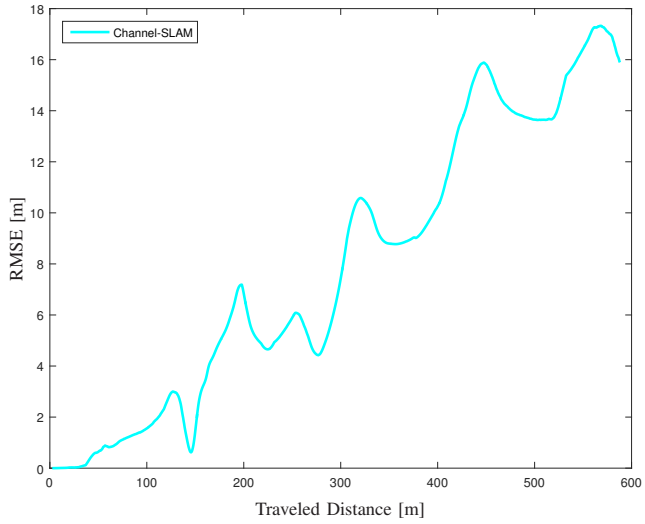

Fig. 8. The RMSE of the receiver versus the receiver traveled distance.

low. Afterwards, the RMSE is increasing during the receiver movement. However, we are still able to estimate the receive position below 18 m after a traveled distance of 600 m. To reduce the overall positioning error, further sensors may be included, e.g., GNSS pseudo range or velocity measurements.

V. CONCLUSION AND OUTLOOK

Within this paper, we presented the idea of Channel-SLAM for ITS applications. We simulated a road user equipped with a circular antenna array consisting of 4 antennas and a gyroscope moving through an urban multipath scenario. Exploiting the multipath components for positioning, the user could be tracked. Future work will contain the creation and exchange of maps of physical and virtual transmitters among

road users. We expect that a-priori maps of transmitters will lead to a faster convergence of the positioning solution as well as a better positioning performance. In particular, the inclusion of VT positions in LDMs will improve the positioning performance in vehicular applications.

VI. Acknowledgement

This work was partially supported by the EU project HIGHTS (High precision positioning for cooperative ITS applications) MG-3.5a-2014-636537 and the DLR project Dependable Navigation.

References

[1] N. Agarwal, J. Basch, P. Beckmann, P. Bharti, S. Bloebaum, S. Casadei, A. Chou, P. Enge, W. Fong, N. Hathi, W. Mann, A. Sahai, J. Stone, J. Tsitsiklis, and B. Van Roy, "Algorithms for gps operation indoors and downtown," *GPS Solutions*, vol. 6, no. 3, pp. 149–160, 2002.

[2] J. Li, Y. Zhao, J. Zhang, R. Jiang, C. Tao, and Z. Tan, "Radio channel measurements and analysis at 2.4/5ghz in subway tunnels," *China Communications*, vol. 12, no. 1, pp. 36–45, Jan 2015.

[3] Y. Shen and M. Win, "On the use of multipath geometry for wideband cooperative localization," in *IEEE Globecom*, Nov. 2009, pp. 1–6.

[4] P. Meissner and K. B. Witrisal, "Multipath-assisted single-anchor indoor localization in an office environment," in *Systems, Signals and Image Processing (IWSSIP), 2012 19th International Conference on*, Apr. 2012, pp. 22–25.

[5] P. Setlur, G. Smith, F. Ahmad, and M. Amin, "Target localization with a single sensor via multipath exploitation," *Aerospace and Electronic Systems, IEEE Transactions on*, vol. 48, no. 3, pp. 1996–2014, Jul. 2012.

[6] C. Gentner, T. Jost, and A. Dammann, "Indoor positioning using time difference of arrival between multipath components," in *IEEE IPIN*, Montbeliard, France, Oct. 2013.

[7] C. Gentner, T. Jost, W. Wang, S. Zhang, A. Dammann, and U.-C. Fiebig, "Multipath Assisted Positioning with Simultaneous Localization and Mapping," *IEEE Trans. Wireless Commun.*, vol. 15, no. 9, pp. 6104–6117, Sep. 2016.

[8] H. Durrant-Whyte and T. Bailey, "Simultaneous localization and mapping: part i," *Robotics Automation Magazine, IEEE*, vol. 13, no. 2, pp. 99–110, June 2006.

[9] T. Jost, W. Wang, U. Fiebig, and F. Perez-Fontan, "Detection and tracking of mobile propagation channel paths," *Antennas and Propagation, IEEE Transactions on*, vol. 60, no. 10, pp. 4875–4883, Oct. 2012.

[10] S. Kay, *Fundamentals of Statistical Signal Processing: Estimation Theory*, ser. Fundamentals of Statistical Signal Processing. Prentice-Hall PTR, 1998.

[11] C. Gentner, R. Pöhlmann, T. Jost, and A. Dammann, "Multipath Assisted Positioning using a Single Antenna with Angle of Arrival Estimations," in *Proceedings of the ION GNSS*, Tampa, FL, USA, Sep. 2014.

[12] B. Ristic, S. Arulampalam, and N. Gordon, *Beyond the Kalman Filter: Particle Filters for Tracking Applications*. Artech House, 2004.

[13] M. Arulampalam, S. Maskell, N. Gordon, and T. Clapp, "A tutorial on particle filters for online nonlinear/non-gaussian bayesian tracking," *Trans. Sig. Proc.*, vol. 50, no. 2, pp. 174–188, Feb. 2002.